Charge exchange in Be^{4+} - $H(n = 1, 2)$ collisions studied systematically by atomic-orbital close-coupling calculations

K Igenbergs[1], J Schweinzer[2] and F Aumayr[1]

[1] Institut für Allgemeine Physik, Technische Universität Wien, Association EURATOM-ÖAW, Wiedener Hauptstr.8-10/E134, A-1040 Vienna, Austria
[2] Max-Planck-Institut für Plasmaphysik, Association EURATOM, Boltzmannstr. 2, D-85748 Garching, Germany

E-mail: `igenbergs@iap.tuwien.ac.at`

Abstract. Charge exchange in Be^{4+} - $H(n = 1, 2)$ collisions was studied using the atomic-orbital close-coupling formalism in its impact parameter description and applying electron translational factors. Calculations were carried out in the energy range of $1 - 750$ keV/amu with fully stripped beryllium ions impacting on atomic hydrogen in its ground state (1s) and in the excited $n = 2$ states. An optimized description of both collision centres was determined by analyzing the convergence of the total cross sections and also by comparison with other theoretical approaches. This optimized description consists of up to 170 basis states involving hydrogen-like states and pseudostates. We present total, n-resolved as well as $n\ell$-resolved cross sections. The latter are needed to evaluate the emission cross sections in two limiting collisional plasma environments, i.e. single-collisional and multi-collisional. The calculated emission cross sections are compared with experimental data from the fusion experiment JET. Taking the experimental environment and certain characteristics of the theoretical methods into account, the agreement can be considered to be quite good.

Submitted to: *J. Phys. B: At. Mol. Phys.*

1. Introduction

Charge exchange (CX) in collision processes between neutral hydrogen isotopes and fully stripped ions has been the subject of a large number of studies in the past (Fritsch & Lin 1991, Bransden et al. 1980). Special interest comes from thermonuclear fusion research since cross sections for these processes are needed for a variety of applications, in particular plasma diagnostics by means of charge exchange recombination spectroscopy (CXRS). CXRS uses spectral line emission following charge exchange between multiply charged ions (e.g. C^{q+}) in the plasma and injected fast neutral atoms, like e.g. H, He, or Li, to measure ion densities (von Hellermann et al. 1990, Schorn et al. 1991, Mandl et al. 1993), temperatures (von Hellermann et al. 1990, Schorn et al. 1992, Mandl et al. 1993), velocities of plasma rotation, and Z_{eff}, the effective charge of the plasma (Isler 1994, Wolfrum et al. 1993, Boileau et al. 1989).

Beryllium (Be) evaporation has been used at the JET (Joint European Torus) tokamak for wall conditioning. After the 2010 shutdown Be-bulk and Be-coated tiles will be used in the JET main chamber for the first wall and the limiters. Tungsten(W)-bulk and W-coated tiles will be used for the divertor and other main wall/limiter regions which are subjected to heat loads too high for Be. A very similar material mix is also foreseen for the plasma facing components of ITER. Due to high erosion of Be, the influx of Be ions into future plasmas of JET and ITER will be high. Be ions in such plasmas will be abundant and therefore CXRS measurements using Be^{4+} promise a high quality determination of the above mentioned plasma parameters. In particular, the precise knowledge of the Be ion concentration (or Be^{4+} density profile) is of considerable importance for transport analysis of such tokamak plasmas. The quality of such concentration measurements heavily relies on the accuracy of the underlying atomic data, namely the CX cross sections. Since energetic hydrogen (deuterium) beams injected into a plasma may contain a certain fraction of excited (metastable) H(2s) atoms, we investigated both

$$Be^{4+} + H(1s) \rightarrow Be^{3+}(n\ell) + H^{+} \tag{1}$$

collisions in the energy range 1-750 keV/amu and

$$Be^{4+} + H(2s) \rightarrow Be^{3+}(n\ell) + H^{+} \tag{2}$$

collisions in the energy range 1-750 keV/amu. Through collisions with plasma particles the original 2s population is statistically redistributed within the $n = 2$ shell. Thus collisions of H(2p) with beryllium have to be taken into account as well:

$$Be^{4+} + H(2p) \rightarrow Be^{3+}(n\ell) + H^{+} \tag{3}$$

The partial $2\ell(m_\ell)$ cross sections then have been added according to their statistical weight

$$\begin{aligned} \sigma(n=2) &= \tfrac{1}{4}\sigma(2s) + \tfrac{3}{4}\sigma(2p) = \\ &= \tfrac{1}{4}\sigma(2s) + \tfrac{1}{4}\left(\sigma(2p0) + \sigma(2p1) + \sigma(2p\text{-}1)\right). \end{aligned} \tag{4}$$

in order to get the cross section for

$$Be^{4+} + H(n = 2) \rightarrow Be^{3+}(n\ell) + H^{+} \tag{5}$$

in a fusion plasma.

Beryllium itself reveals a number of remarkable features in its spectrum. The diagnostic scope is vast but requires elaborate atomic modeling for its exploitation. Fully stripped Be ions generally occur in a plasma at high temperatures. Through CX with neutral hydrogen isotopes excited $(Be^{3+})^*$ ions are formed, which then deexcite via emission of photons some of which are in the visible spectral region. Setting the viewing lines of the spectrometers detection this radiation to the plasma centre ensures that they do originate from ions formed through CX and not simply through ionization. The high principal numbers of the active electron support this analysis. (Isler 1994, Boileau et al. 1989)

We start with a short description of the used theoretical approach, then continue with the description of employed basis sets and close with a detailed analysis of the calculated cross sections. Atomic units are used unless otherwise stated.

2. Theory & calculations

For calculating cross sections of reactions (1), (2), and (3), we used the well known atomic-orbital close-coupling (AOCC) formalism (Fritsch & Lin 1991, Bransden & McDowell 1992) in its impact parameter description. In this semiclassical approach, the total electron wavefunctions are expanded into target- and projectile-centred traveling atomic orbitals (AO). The time-dependent Schrödinger equation is solved in the truncated Hilbert space following the procedure by (Nielsen et al. 1990).

The appropriate choice of atomic basis states reflects the physical problem that is to be treated. The basis sets, however, have commonly been sought to meet certain requirements of physics and convenience. All significant initial and final states should be included as well as a sufficient number of intermediate states. Furthermore, the basis sets should be easy to generate (Fritsch & Lin 1991).

The simplest wavefunctions are derived from the solution of the Schrödinger equation of the hydrogen atom and thus use Laguerre-type radial parts and spherical harmonics as angular parts.

$$\varphi(\vec{r}) \quad = R_{n\ell}(r) Y_{\ell m}(\Omega) \tag{6}$$

$$R_{n\ell}(r) = \sqrt{\left(2 \cdot \frac{Z}{n}\right)^3 \cdot \frac{(n-1)!}{2n\,[(n+\ell)!]}} \cdot e^{-r \cdot \frac{Z}{n}} \cdot \left(2r \cdot \frac{Z}{n}\right)^{\ell} L_{n-\ell-1}^{2\ell+1}\left(2r\frac{Z}{n}\right) \tag{7}$$

where Z is the atomic number, $L_{n-\ell-1}^{2\ell+1}$ are the Laguerre polynomials. This type of wavefunction is certainly the most appropriate for one-electron systems such as Be^{4+} + H. Both the target and the projectile centre need to be sufficiently described through expansions using these basis wave functions.

The calculations are done in the so-called collision frame (b parallel to x-axis, v parallel to the quantization axis z). Real spherical harmonics are used for the angular part of the basis states. With this choice only states with the same symmetry with respect to a reflection on the scattering plane couple in the AOCC approach. Thus calculations with an initial state of positive reflection symmetry do not couple with states of negative reflection symmetry and vice versa leading to basis states of minimal size. In particular, the basis sets using the "collision frame" for calculations with initial states of negative reflection symmetry become small because all states with positive reflection symmetry can be omitted.

All the calculations were performed on an impact parameter mesh ($0.1 \leq b \leq 10.0$) which was chosen to be more closely meshed at smaller impact parameters. The total cross section is calculated via

$$\sigma_{tot} = \sum_{n\ell} \sigma_{n\ell} = 2\pi \sum_{n\ell} \int bP_{n\ell}(b)db \tag{8}$$

where $\sigma_{n\ell}$ is the state-selective cross section and $P_{n\ell}$ the probability for the electron being in the $Be^{3+}(n\ell)$ final state.

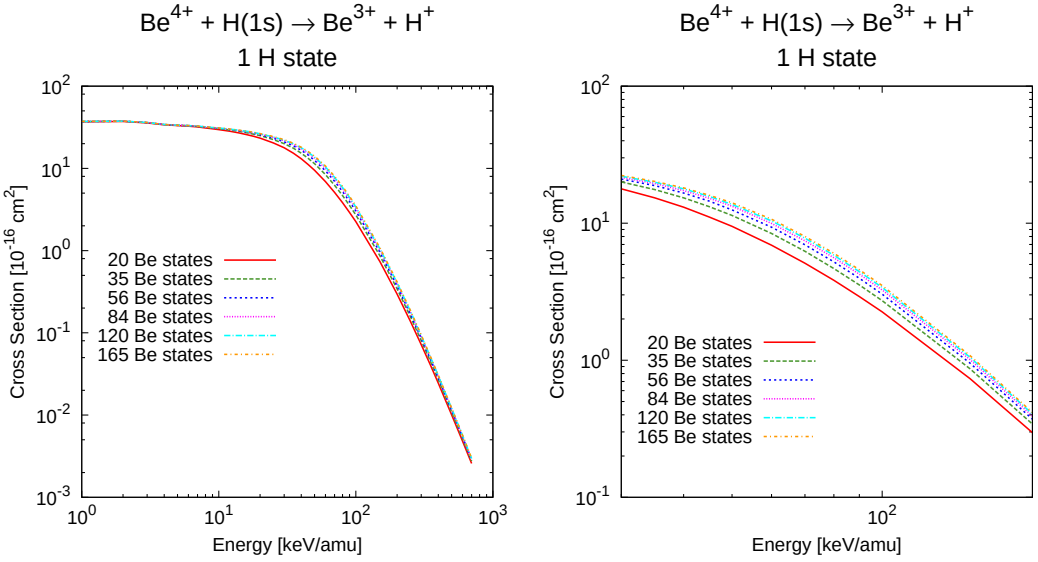

Figure 1. Color online. Comparison of various basis sets employing only one single target state (H(1s)) and various numbers of projectile states still omitting pseudo continuum states. (a) Shows the total cross section over the whole energy range (1 - 750 keV/amu) used in our calculations. (b) Shows an enlarged part of (a) of the energy region between 30 - 200 keV/amu.

Fig.1 shows a number of calculations employing only one single state on the H centre (H(1s)) and only purely hydrogen-like states on the Be centre. The maximum principal quantum numbers range from $n^{Be}_{max} = 4$, (20 states), to $n^{Be}_{max} = 9$, (165 states). It can be seen that the cross sections converge toward higher n. The difference between

$n_{max}^{Be} = 8$ and $n_{max}^{Be} = 9$ is negligibly small so that the additional 45 states are not necessary for good, convergent calculations.

These configurations don't take into account that other processes than CX, i.e. ionization or excitation, might happen when a fully stripped ion impacts on atomic hydrogen. Thus, ionization and target excitation channels need to be added to the description of the centres. The inclusion of target excitation processes is achieved by adding excited H($n\ell$)- and suitable pseudo-states. We first started to look for an ideal configuration of the H centre, see Fig.2(a), which we found using eight basis states. Four pure H states ($|Z; nlm\rangle = |1.0; 100\rangle; |1.0; 200\rangle; |1.0; 210\rangle; |1.0; 211\rangle$) and four pseudostates ($|Z; nlm\rangle = |1.4; 100\rangle; |2.4; 200\rangle; |2.4; 210\rangle; |2.4; 211\rangle$).

Comparing both calculations with classical trajectory Monte-Carlo (CTMC) calculations from (Illescas & Riera 1999) and taking into account that the CTMC description of charge exchange processes is quite accurate at high energies shows that the H centre is indeed better described using this more complex expansion.

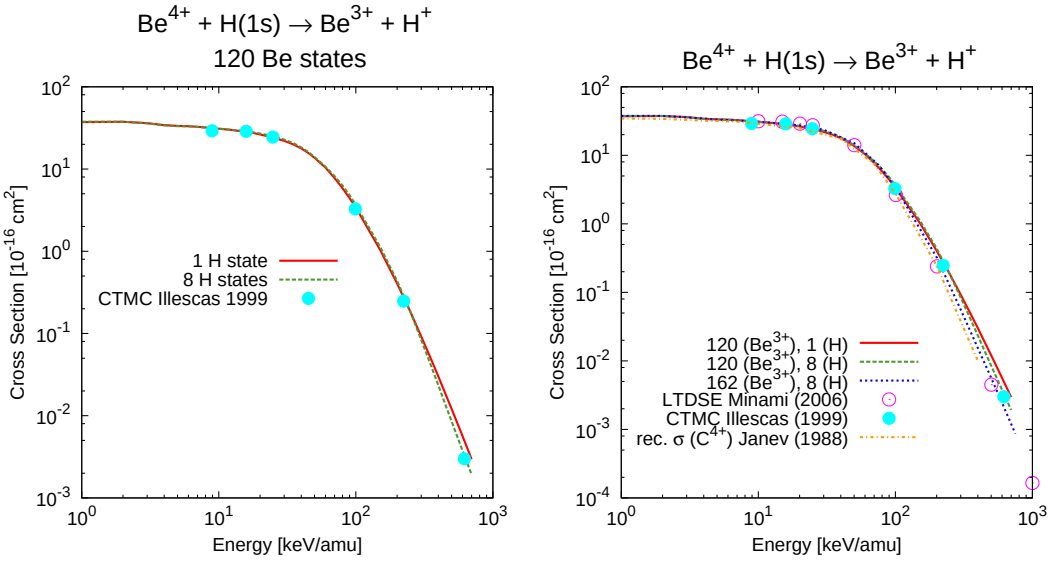

Figure 2. Color online. Search for the best description of (a) the H centre. 8 basis states consisting of 4 hydrogen states and 4 pseudostates (with Z = 1.4 and Z=2.4) form a very good expansion of the wavefunction of the target atom. For comparison CTMC data from (Illescas & Riera 1999) are shown. (b) the Be centre. Calculations applying 120 ($n \leq 8$) and 162 ($n \leq 8$ & UA) are compared. For comparison also data from (Minami et al. 2006, Illescas & Riera 1999) are shown, as well as the recommended cross section for $C^{4+} - H(1s)$ from (Janev et al. 1988)

Now, to include ionization in our description we used a number of pseudostates on the Be centre. These pseudostates are not "physical states" associated with a direct interpretation like atomic orbital, but they are needed to describe the continuum (Fritsch & Lin 1991). The eigenvalues of these pseudostates are determined by diagonalizing the Hamiltonian on the Be centre. Positive eigenvalues correspond to unbound pseudostates.

We applied Slater-type orbitals (STOs), namely we used united atom (UA) states with $Z = 5.0$. The most ideal configuration of UA states on the Be centre includes 42 states which comprise of full $n = 2$ and $n = 3$ shells, UA(4d) and UA(4f), and principal quantum numbers $5 \leq n \leq 8$ and the highest allowed values of the corresponding azimuthal quantum numbers $\ell = n - 1$.

The inclusion of these 42 UA states on the Be centre, which also include ionization channels with eigen-energies $\varepsilon > 0$, ameliorates the description of the processes on the Be centre significantly, see Fig.2(b). Our AOCC calculations are compared with two different theoretical approaches, the already previously mentioned CTMC approach (Illescas & Riera 1999) and the lattice, time-dependent Schrödinger equation (LTDSE) approach (Minami et al. 2006), as well as recommended cross sections for charge exchange between C^{4+} and H(1s) (Janev et al. 1988). Fig.2(b) compares the total cross sections and it can be seen that our AOCC calculations coincide perfectly with all other approaches at low and medium energies. At energies above 100 keV/amu our calculations lie in between the CTMC and the LTDSE calculations. There is a number of other studies of this collisional system, e.g. (Lüdde & Dreizler 1982). They are not shown in fig.2 to keep the plot from overflowing with data points. They generally agree well with our calculations as well as the shown data from (Minami et al. 2006, Illescas & Riera 1999).

For H($n = 2$) as donor atom, we started out with the optimized basis described above. It turned out that a few energetically low lying basis states could be removed. The optimized description of the H centre consist of the same 8 basis states as above. On the Be centre, we removed all states with principal quantum numbers $n = 1$ and $n = 2$. The optimized basis on the Be centre now comprises of 155 states. The impact parameter mesh had to be adapted as well, in particular the mesh was tightened below $b = 3.0$. The initial state was switched to either H($2s$), H($2p0$), H($2p1$), or H($2p - 1$).

Fig.3 shows our results compared to three different theoretical approaches, namely a semi-classical approach using a molecular orbital expansion of the wavefunctions (Errea et al. 1998), Landau-Zener calculations (Casaubon 1993), and CTMC (Hoekstra et al. 1998). The different theoretical approaches differ sometimes quite profoundly. The complexity of all sorts of calculations involving the $n = 2$ shell of the hydrogen atom and considering the highly excited main capture channel ($Be^{3+}(n = 5)$ makes the observed deviations between the approaches not overly surprising. The molecular expansion of (Errea et al. 1998), which results in larger cross is expected to be more suitable in lower energy ranges. Our calculations roughly follow the CTMC calculations by (Hoekstra et al. 1998).

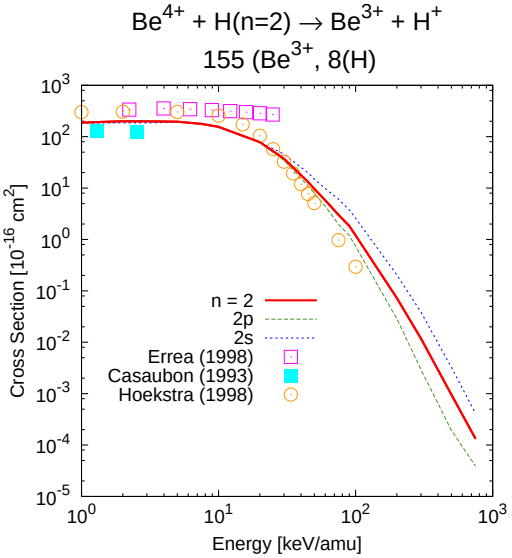

Figure 3. Color online. Cross sections for Be^{4+} impacting on an excited $H(n = 2)$ target in the energy range (1 - 750 keV/amu). Cross sections of the various subshells are shown as well. For comparison data for H(2s) targets of semi-classical calculations using an expansion of wavefunctions into molecular orbitals (Errea et al. 1998), calculations using the Landau-Zener method (Casaubon 1993), and for an $H(n = 2)$ target from CTMC calculations (Hoekstra et al. 1998) are shown.

3. Detailed analysis of cross sections with optimized description of collision centres

3.1. State selective cross sections

For the analysis of CXRS data, not total but state selective cross sections $\sigma^{CX}(n\ell)$ are needed. In the AOCC approach the state-selective cross sections are calculated via

$$\sigma(n\ell) = 2\pi \int P_{n\ell} bdb = 2\pi \int |a_{n\ell}|^2 bdb \tag{9}$$

where $P_{n\ell}$ are the transitions probabilities and $a_{n\ell}$ are the respective probability amplitudes. The total cross section is given by the sum over all transitions into bound states, i.e. those with negative eigenvalues. Subsequently, cross sections for capture into a particular n-shell are defined as follows:

$$\sigma_n^{CX} = \sum_\ell \sigma_{n\ell}^{CX} \tag{10}$$

Fig.4 compares the n-resolved cross sections. At energies below 50 keV/amu capture from H(1s) into $Be^{3+}(n = 3)$ is most prominent, followed by capture into the $n = 4$ and $n = 5$ shells. Capture from $H(n = 2)$ into $Be^{3+}(n = 5)$ is most prominent, followed by capture into the $n = 6$ and $n = 7$ shells. Towards high impact energies the population of final n-shells follows more and more the well-known $1/n^3$ distribution (Coleman & Trelease 1968).

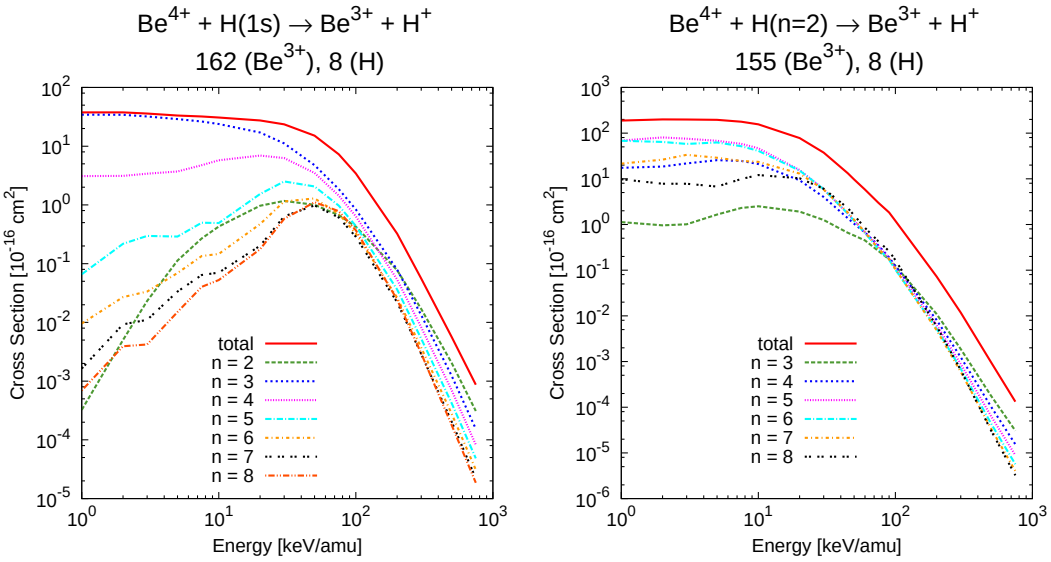

(a) (b)

Figure 4. Color online. Comparison of n resolved cross sections (a) for a H(1s) target applying an expansion which uses 8 basis states on the H centre and 162 basis states on the Be centre and (b) for a H($n = 2$) target applying 8 basis states on the H centre and 155 basis states on the Be centre.

The wavelengths of the respective deexcitation lines, $j \rightarrow i$, can be calculated using

$$\frac{1}{\lambda} = R_H \cdot Z^2 \cdot \left(\frac{1}{n_j^2} - \frac{1}{n_i^2} \right). \tag{11}$$

with R_H being the Rydberg constant. The values calculated using (11) are shown in Tab.1 and correspond to the values found in the Grotian diagrams (Bashkin & Stoner 1978). The wavelength of two transitions ($6 \rightarrow 5$ and $8 \rightarrow 6$) are in the visible range and thus most convenient for CXRS from an experimental point of view, e.g. suitability for fiber optics.

Δn = 1			**Δn = 2**		
n_j	**n_i**	**λ[nm]**	**n_j**	**n_i**	**λ[nm]**
2	1	7.6	3	1	6.4
3	2	41	4	2	30.4
4	3	117	5	3	80.1
5	4	253	6	4	164.0
6	5	466	7	5	290.7
7	6	773	8	6	468.7
8	7	1191	9	7	706.4

Table 1. Wavelength of the lines $n \rightarrow n-1$ and $n \rightarrow n-2$ in the spectrum of Be^{3+}. The spectral line of the $6 \rightarrow 5$ and the $8 \rightarrow 6$ transition are in the visible range. Thus, they are the convenient choice for CXRS.

Now, we take a closer look at the state-selective cross sections $\sigma(n = 6)$ and $\sigma(n = 8)$ in terms of nℓ-resolved cross sections. For Be4+ + H(1s) collisions, the

cross sections show very similar characteristics, see fig.5(a) and fig.5(b). The maximum is mostly located around $30 - 50$ keV/amu. The cross sections for capture into $\ell = 2$ (d-shell) are most prominent both for $n = 6$ and $n = 8$ around the peak between 20 keV/amu and 100 keV/amu.

For impact on H($n = 2$), see fig.5(c) and fig.5(d), the characteristics are not as prominent as for the H(1s) target. It can be seen though, that the capture cross sections are larger by up to an order of magnitude.

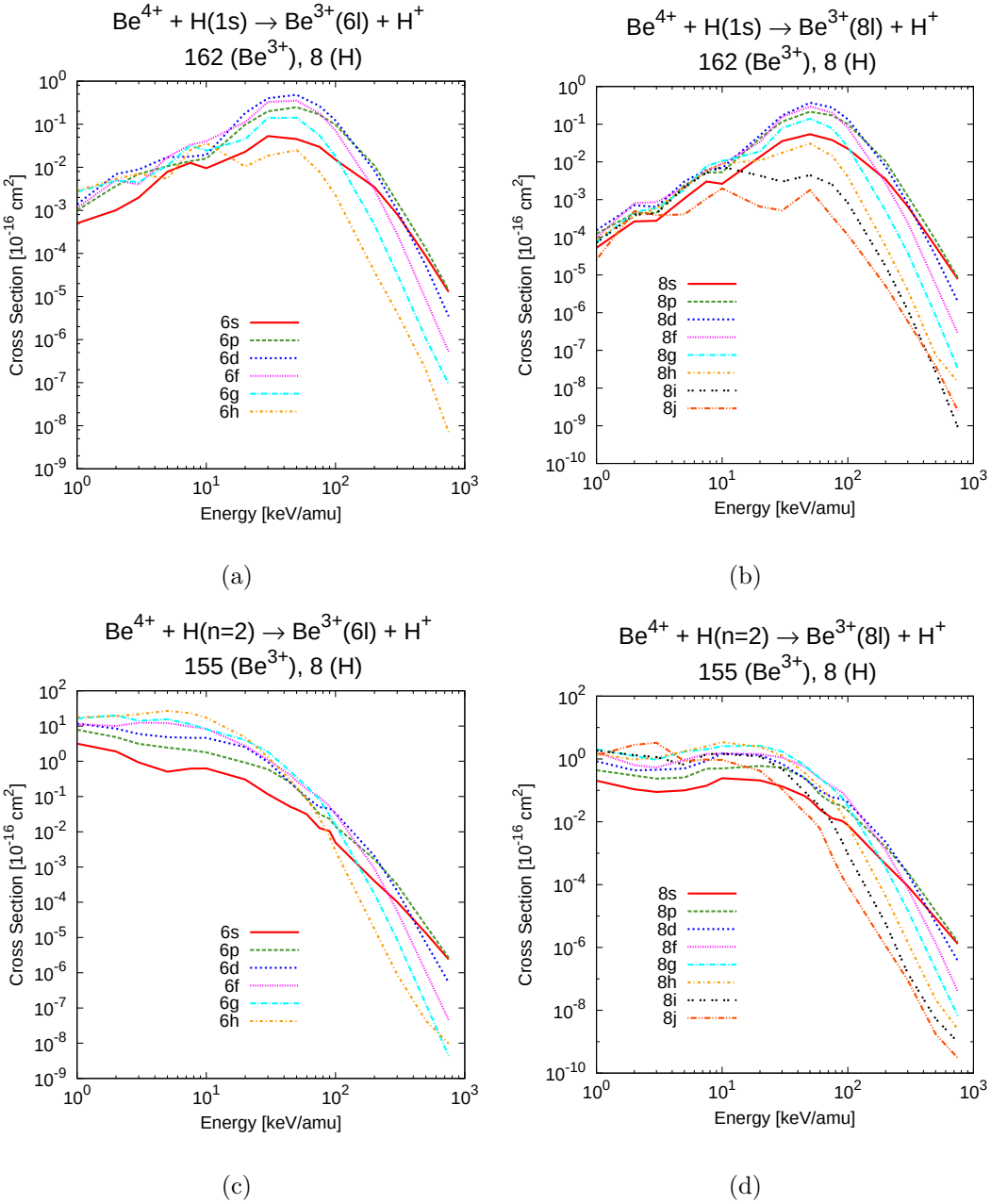

Figure 5. Color online. nℓ resolved cross sections. (a) H(1s) target, $n = 6$ (b) H(1s) target, $n = 8$ (c) H($n = 2$) target, $n = 6$ (d) H($n = 2$) target, $n = 8$

3.2. Emission cross sections & effective emission coefficients

The emission cross section for a transition $n_i \rightarrow n_f$ is given by

$$\sigma^{emi}_{n_i \rightarrow n_f} = \sum_{\ell_i,\ell_f} \sigma^{emi}_{n_i\ell_i \rightarrow n_f\ell_f} = \sum_{\ell_i,\ell_f} \sum_{n \geq n_i} \sum_{\ell=0}^{n-1} c_{n\ell}\sigma_{n\ell} \tag{12}$$

where $c_{n\ell}$ is the contribution of the $n\ell$ level to the $n_i\ell_i \rightarrow n_f\ell_f$ transition. These contributions can be calculated recursively via

$$c_{n\ell} = \sum_{n'=n_i}^{n-1} \sum_{\ell'=0}^{n'-1} b_{n\ell \rightarrow n'\ell'} c_{n'\ell'} \left[\delta_{\ell'(\ell-1)} + \delta_{\ell'(\ell+1)}\right] \tag{13}$$

$$c_{n_i\ell_i} = b_{n_i\ell_i \rightarrow n_f\ell_f} \tag{14}$$

where $b_{n\ell \rightarrow n'\ell'}$ are the branching ratios, which are defined using A_{21}, the Einstein coefficient for spontaneous emission, and the lifetime of the state τ

$$b_{n\ell \rightarrow n'\ell'} = A_{21}(n\ell \rightarrow n'\ell')\tau(n\ell) = \frac{A_{21}(n\ell \rightarrow n'\ell')}{\sum_{\ell'} A_{21}(n\ell \rightarrow n'\ell')} \tag{15}$$

The effective emission coefficients q are defined as the emission cross sections averaged over a velocity distribution:

$$q^{eff}_{n_i \rightarrow n_f} = \langle \sigma^{emi}_{n_i \rightarrow n_f} v \rangle \tag{16}$$

In first approximation, the level population can be considered to result only from primary processes, as in this case charge exchange recombination. Additionally, secondary processes like the redistribution of the populations through l-mixing collisions and cascade effects have to be taken into account.

We derived the emission cross sections for these two limiting cases, i.e. for single- and multi-collisional environments. In both cases, we calculate the cascade contributions of the various $n\ell$-levels to the emission line using (14). When considering a multi-collisional environment where the level populations are statistically redistributed, the redistribution must inherently include all cascade contributions to the level in question.

The first case considers a single collision environment and simply uses the $n\ell$-resolved cross sections $\sigma^{singlecoll.}_{n\ell} = \sigma^{AOCC}_{n\ell}$ as calculated by our program, the second estimates a multi-collisional environment and therefore uses a statistical redistribution of the ℓ-level population within a certain n-shell.

$$\sigma^{stat}_{n\ell} = \frac{2\ell+1}{n^2}\sigma_n = \frac{2\ell+1}{n^2} \sum_{\ell} \left(\sigma^{AOCC}_{n\ell} + \sigma^{casc}_{n\ell}\right) \tag{17}$$

where $\sigma^{casc}_{n\ell}$ are the cascade contributions to the $n\ell$-level by higher levels.

Fig.6 compares the effective emission coefficients of the various visible spectral lines for both scenarios and also with data for the $6 \rightarrow 5$ line on the basis of a CTMC treatment of the collision (Hoekstra et al. 1998) and with data from (Summers et al. 1992). Figs.6(a) and 6(b) treat a H(1s) target, whereas figs.6(c) and 6(d) use H($n = 2$) as

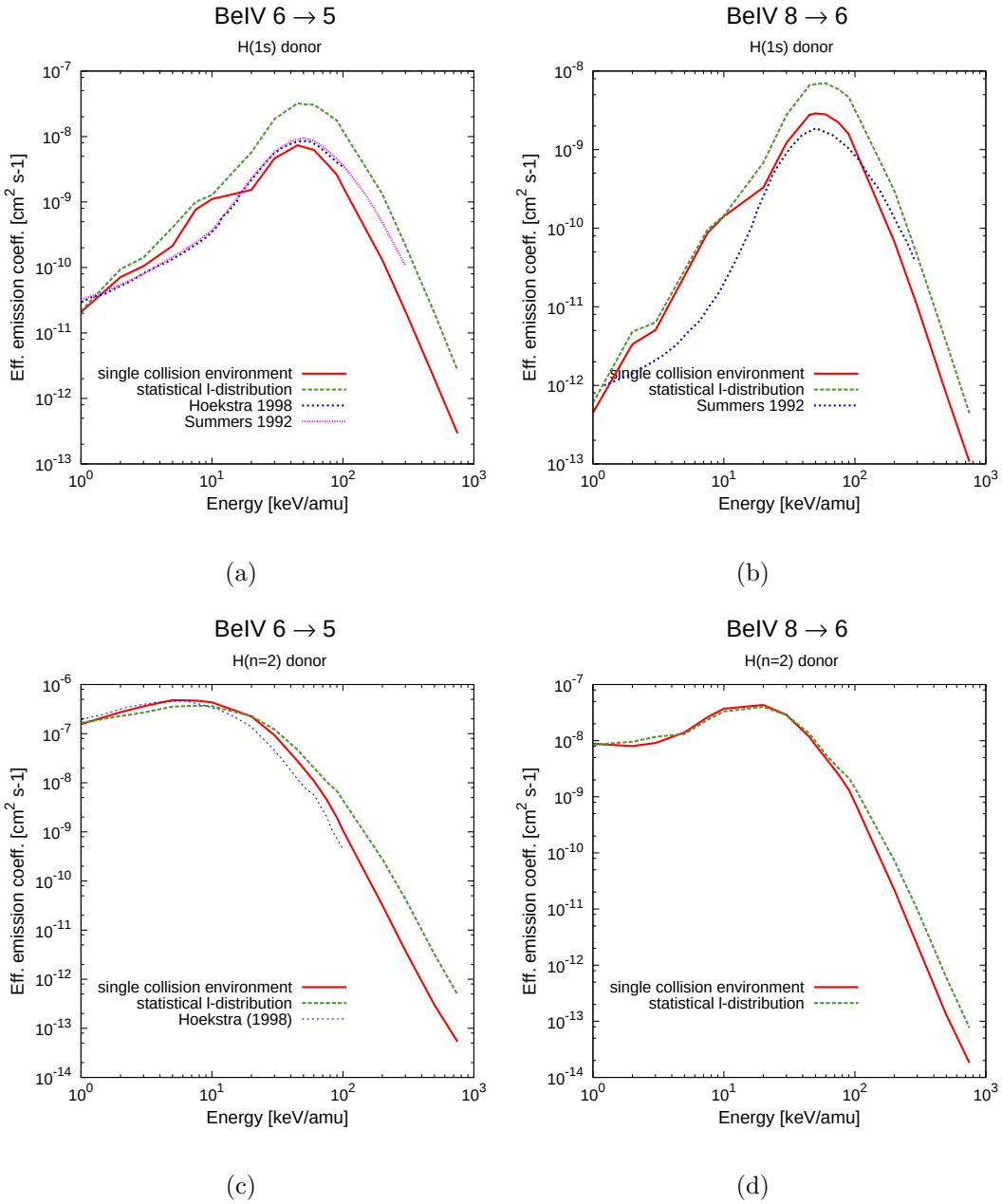

Figure 6. Color online. Effective emission coefficients of the two major visible lines in the Be^{3+} spectrum calculated from cross sections using the above described optimized descriptions of the collision centres. (a) The $6 \rightarrow 5$ transition for an H(1s) donor. (b) The $8 \rightarrow 6$ transition for an H(1s) donor. (c) The $6 \rightarrow 5$ transition for an H($n = 2$) donor. (d) The $8 \rightarrow 6$ transition for an H($n = 2$) donor. Our data are compared to data by (Hoekstra et al. 1998) and (Summers et al. 1992)

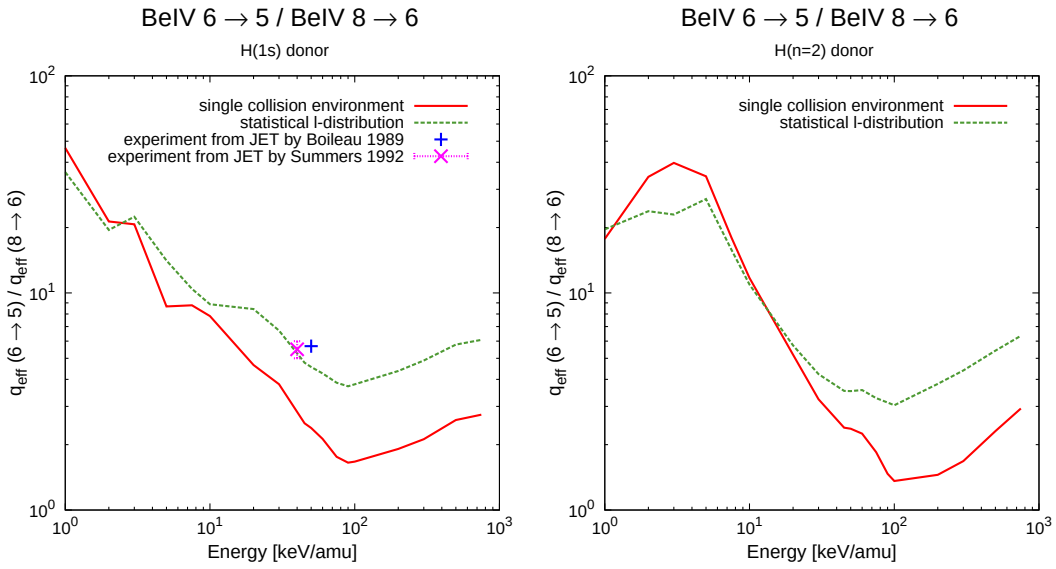

(a) (b)

Figure 7. Color online. The ratio of the $6 \rightarrow 5$ line and the $8 \rightarrow 6$ line are compared for a single collision environment (red), a multi-collisional environment (green). The experimental value from JET by Boileau et al. (Boileau et al. 1989) is marked with a cross and the one from Summers et al. (Summers et al. 1992) with an x (a) for an H(1s) donor atom. (b) for an H($n = 2$) donor atom.

target atom. Between 20 keV/amu and 100 keV/amu, our estimation of the $6 \rightarrow 5$ line (H(1s) donor) in a single-collision environment agrees quite well with the CTMC based coefficients. For an H($n = 2$) donor the coefficients show a very good agreement between 1 keV/amu and 20 keV/amu.

In Fig. 7, we compare the ratios of the emission coefficients in single- and multi-collisional environments with experimental values from JET from (Boileau et al. 1989) and (Summers et al. 1992). The agreement between the experimental values and our calculations is satisfactory. It is also evident that the experimental values are very close to the statistical ℓ-distribution which is to be expected since a fusion plasma is a multi-collisional environment.

4. Conclusions

In this paper we have presented charge exchange cross sections for fully stripped Be ions impacting on H($n = 1, 2$). First, impact on ground state hydrogen was studied to find a convergent basis set, later this basis set was slightly adapted to calculate impact on H(2s, 2p0, 2p1, 2p-1) as well. These cross sections were averaged to represent impact on H($n = 2$) in a fusion plasma environment.

In the second part of this paper, the calculations using the optimized basis sets and optimized impact parameter meshes were used to derive emission cross sections and effective emission coefficients relevant for CXRS diagnostic experiments in fusion

plasmas. Despite simplistic assumptions about the plasma environment good agreement with experimentally observed line emission values is achieved.

5. Acknowledgments

Katharina Igenbergs is a DOC-fFORTE-fellow of the Austrian Academy of Sciences at the Institute of General Physics at Vienna University of Technology.

This work, supported by the European Communities under the Contract of Association between EURATOM and the Austrian Academy of Sciences, was carried out within the framework of the European Fusion Development Agreement. The views and opinions expressed herein do not necessarily reflect those of the European Commission.

6. References

Bashkin S & Stoner J O 1978 *Atomic energy-levels and Grotrian diagrams. Volume I. Hydrogen I - Phosphorus XV* North-Holland Publishing Company Amsterdam, New York, Oxford.

Boileau A, von Hellermann M, Horton L, Spence J & Summers H 1989 *Plasma Phys. & Contr. Fusion* **31**(5), 779 – 804.

Bransden B H, Newby C W & Noble C J 1980 *Journal of Physics B: Atomic and Molecular Physics* **13**(21), 4245–4255.
URL: *http://stacks.iop.org/0022-3700/13/4245*

Bransden B & McDowell M 1992 *Charge-Exchange and the Theory of Ion-Atom Collisions* Vol. 82 of *The International Series of Monographs on Physics* Oxford Science Publications.

Casaubon J I 1993 *Phys. Rev. A* **48**(5), 3680–3683.

Coleman J P & Trelease S 1968 *Journal of Physics B: Atomic and Molecular Physics* **1**(2), 172–180.
URL: *http://dx.doi.org/10.1088/0022-3700/1/2/306*

Errea L F, Harel C, Jouin H, Mendez L, Pons B & Riera A 1998 *Journal of Physics B: Atomic, Molecular and Optical Physics* **31**(16), 3527–3545.
URL: *http://stacks.iop.org/0953-4075/31/3527*

Fritsch W & Lin C 1991 *Physics Reports (Review Section of Physics Letters)* **202**, 1–97.

Hoekstra R, Anderson H, Bliek F, von Hellermann M, Maggi C, Olson R & Summers H 1998 *Plasma Phys. & Contr. Fusion* **40**, 1541–1550.

Illescas C & Riera A 1999 *Phys. Rev. A* **60**(6), 4546–4560.

Isler R 1994 *Plasma Physics and Controlled Fusion* **36**, 171–208.

Janev R, Phaneuf R & Hunter H 1988 *Atomic Data & Nuclear Data Tables* **40**, 249–281.

Lüdde H J & Dreizler R M 1982 *Journal of Physics B: Atomic and Molecular Physics* **15**(16), 2713–2720.
URL: *http://dx.doi.org/10.1088/0022-3700/15/16/019*

Mandl W, Wolf R C, von Hellermann M G & Summers H P 1993 *Plasma Physics and Controlled Fusion* **35**(10), 1373–1394.
URL: *http://stacks.iop.org/0741-3335/35/1373*

Minami T, Pindzola M & Schultz D 2006 *J. Phys. B: At. Mol. Phys* **39**, 2877 – 2891.

Nielsen S E, Hansen J P & Dubois A 1990 *Journal of Physics B: Atomic, Molecular and Optical Physics* **23**(15), 2595–2612.
URL: *http://stacks.iop.org/0953-4075/23/2595*

Schorn R P, Hintz E, Rusbldt D, Aumayr F, Schneider M, Unterreiter E & Winter H 1991 *J. Appl. Phys. B: Lasers & Optics* **52**(2), 71–78.

Schorn R, Wolfrum E, Aumayr F, Hintz E, Rusbuldt D & Winter H 1992 *Nuclear Fusion* **32**(3), 351–9.
URL: *http://stacks.iop.org/0029-5515/32/351*

Summers H P, Dickson W J, Boileau A, Burke P G, Denne-Hinnov B, Fritsch W, Gianella R, Hawkes N C, von Hellermann M, Mandl W, Peacock N J, Reid R, Stamp M F & Thomas P R 1992 *Plasma Physics and Controlled Fusion* **34**(3), 325–352.
URL: *http://stacks.iop.org/0741-3335/34/325*

von Hellermann M G, Mandl W, Summers H P, Weisen H, Boileau A, Morgan P D, Morsi H, Koenig R, Stamp M F & Wolf R 1990 Vol. 61 AIP pp. 3479–3486.
URL: *http://link.aip.org/link/?RSI/61/3479/1*

Wolfrum E, Aumayr F, Wutte D, Winter H, Hintz E, Rusbüldt D & Schorn R P 1993 *Review of Scientific Instruments* **64**(8), 2285–2292.
URL: *http://link.aip.org/link/?RSI/64/2285/1*